# Supplemental Information

## Supplemental Results

### Manual curation and expansion of Model SEED draft reconstruction iFpraus_v0.1

The draft reconstruction generated by Model SEED (1), iFpraus_v0.1, consisted of 820 reactions, 874 metabolites and 598 genes. 649 reactions were blocked and could thus not carry flux, and 20 non-spontaneous metabolic and transport reactions were not gene-associated and thus filled in during the auto-completion step of the Model SEED pipeline.

**Translation of Model SEED identifiers**

Model SEED reaction and metabolite identifiers included in the draft reconstruction were replaced with standardized BiGG (2) nomenclature. As *F. prausnitzii* is not yet included in the NCBI Gene database, we replaced the Model SEED gene identifiers included in iFpraus_v0.1 with the appropriate NCBI Protein identifiers.

**Biomass objective function**

As information on *F. prausnitzii*'s biomass composition is currently mostly unavailable, the stoichiometric values for vitamins, cofactors, minerals and amino acids included in the template biomass objective function included in the Model SEED draft reconstruction were kept. The template biomass function is based on a curation of the biomass objective functions in 19 published reconstructions (1) and may thus not correspond well to the true biomass composition of *F. prausnitzii*. Based on the limited available data, fatty acids included in the biomass objective function were modified and the biomass precursor spermidine was removed (see below). Once more detailed information on the biomass composition of *F. prausnitzii* becomes available, the biomass objective function will be modified accordingly.

## Gap-filling of central pathways

As few reactions as possible were included without any genomic and biochemical support. Consequently, only 5 non-spontaneous metabolic reactions were included without supporting evidence. Reactions representing DNA replication, transcription and protein biosynthesis were removed, as they are considered to be outside the scope of metabolic reconstructions. This led to the removal of 126 genes.

## Fermentation pathways

While universal pathways such as glycolysis were well-represented in iFpraus_v0.1, *F. prausnitzii*'s species-specific butyrate production pathways were constructed manually. The key enzyme for butyrate production is butyryl-CoA: acetate CoA-transferase (FAEPRAA2165_01575, assigned reaction ID BTCOAACCOAT). This enzyme consumes acetate to produce butyrate and acetyl-CoA from butyryl-CoA, thus explaining the growth-promoting effect of acetate consumption (3). Pyruvate can be either fermented to D-lactate by D-lactate dehydrogenase (FAEPRAA2165_01388, BiGG ID: LDH_D) or to formate by pyruvate-formate lyase (FAEPRAA2165_02890 and FAEPRAA2165_02891, BiGG ID: PFL), or converted to acetyl-CoA by pyruvate:ferredoxin oxidoreductase (FAEPRAA2165_00243, BiGG ID: POR4i). Butyryl-CoA is formed from acetyl-CoA via acetoacetyl-CoA, 3-hydroxybutyryl-CoA and crotonyl-CoA, yielding reduction equivalents in the form of NADH (FAEPRAA2165_01578-01581, BiGG IDs: ACACT1r, HACD1, ECOAH1, assigned ID BTCOADH). Further energy is conserved through the buildup of a proton gradient via a membrane-associated NADH: ferredoxin oxidoreductase (FAEPRAA2165_02985-_02990 and FAEPRAA2165_02634-02635, assigned ID FDNADOX_H) (4). *F. prausnitzii* possesses an extracellular electron shuttle via flavins and thiols with extracellular oxygen or intracellular fumarate serving as terminal electron

acceptors. Riboflavin and either L-cysteine or glutathione are required for this shuttle to be functional (5). Appropriate reactions (assigned IDs ESHCYS_FPe, ESHCYS2_FPe, ESHGLU_FPe, ESHGLU_FPe) were added to iFpraus_v0.1. The extracellular electron shuttle from cysteine/ glutathione to oxygen via riboflavin was assumed to be nonenzymatic. Furthermore, an extracellular flavin reductase (FAEPRAA2165_00362, assigned ID FLVRxe) was included to enable flux through the shuttle.

We then attemped to identify an intracellular electron transport chain in *F. prausnitzii* A2-165 by searching for genes with sequence similarity to the cytochrome c oxidase of the *Lachnospiraceae* representative *Roseburia intestinalis* M50/1 (ROI_15070) in its genome. A BLASTP score of 29.3 and an e-value of 0.28 were calculated for the closest match, FAEPRAA2165_00652, which is annotated as a hypothetical protein. A2-165 thus likely does not possess a cytochrome c oxidase.

**Amino acid metabolism**

The draft reconstruction iFpraus_v0.1 contained complete synthesis pathways for L-threonine, L-valine, L-leucine, L-isoleucine, L-lysine, L-histidine, L-arginine, glycine, L-proline, L-glutamate, L-glutamine, L-aspartate, and L-asparagine based on the genome sequence. Tryptophan biosynthesis is not annotated in the genome and *F. prausnitzii* does not produce indole (6), and it is thus unlikely that *F. prausnitzii* can synthesize this amino acid. As L-alanine transaminase is not annotated in the *F. prausnitzii* genome, the reconstruction currently predicts that L-alanine cannot be formed *de novo*. According to annotation, serine cannot be synthesized from 3-phosphoglycerate, and by association, L-cysteine synthesis depends on an external serine and hydrogen sulfide source. L-phenylalanine and L-tyrosine were initially predicted essential due to chorismate mutase not being present in the reconstruction. A gene encoding chorismate mutase (FAEPRAA2165_00020, BiGG ID:

CHORM) was later identified and L-phenylalanine and L-tyrosine are thus no longer essential in the final reconstruction iFpraus_v1.0.

The chemically defined medium proposed by iFpraus_v0.2, CDM1 (Figure 1) contained L-alanine, L-cysteine, L-methionine, L-serine, L-phenylalanine, L-tyrosine, and L-tryptophan. No growth was observed unless a mix of 11 additional amino acids was supplemented, indicating that some of the annotated amino acid biosynthesis pathways may be nonfunctional or insufficient. Further curation of the model will have to be performed once the amino acid requirements of the microbe become known.

The microbe is predicted to synthesize putrescine, but not spermidine, as adenosylmethionine decarboxylase is not annotated for *F. prausnitzii*. The biomass objective function contained spermidine. As *F. prausnitzii* grew without spermidine in medium in our *in vitro* experiments, either the polyamine is not required or a not yet annotated pathway exists for its synthesis. Assuming that it is nonessential, spermidine was removed from the biomass objective function.

**Pyrimidine and purine metabolism**

Pyrimidine and purine metabolism was mostly accounted for based on genome annotation, except that iFpraus_v0.1 was unable to synthesize all trinucleotides from the respective dinucleotides. GTP synthesis was enabled by including an additional reaction of adenylate kinase (FAEPRAA2165_02826, BiGG ID: ADK3). No enzyme performing net synthesis of UTP and dTTP from the respective dinucleotides could be identified in the *F. prausnitzii* genome. Thus, it was necessary to include nucleoside-diphosphate kinase (BiGG IDs: NDPK2, NDPK4) despite the lack of genomic support for the presence of this enzyme.

**Fatty acid metabolism**

*F. prausnitzii* belongs to the gram-positive *Clostridium leptum* group, but usually stains gram-negative (6) and thus may not produce teichoic acid, which was thus not included in the reconstruction. The microbe does not possess hydroxy fatty acids and the main fatty acids are saturated and unsaturated up to a length of 18 carbons (7). In the lack of other information about *F. prausnitzii*'s fatty acid composition, we removed all hydroxy fatty acid synthesis reactions included in the draft reconstruction (123 in total) and added all fatty acids shown to be present (7) to the biomass objective function. Hydroxy fatty acids are included in the template biomass objective function routinely added to every Model SEED draft reconstruction (1) and are likely not found in every microbe. No genes involved in fatty acid synthesis were removed.

Knowledge on *F. prausnitzii*'s cell wall structure is currently lacking. A putative capsular polysaccharide biosynthesis reaction (assigned ID CPSS_FP) was formulated based on *Streptococcus anginosus*, another *Firmicutes* representative, consisting of glucose, galactofuranose, N-acetylgalactosamine, and L-rhamnose (8). At least seven genes predicted to be involved in capsular polysaccharide biosynthesis are annotated in *F. prausnitzii* A2-165's genome (FAEPRAA2165_00974-00975, FAEPRAA2165_00979, FAEPRAA2165_00986, FAEPRAA2165_00988, FAEPRAA2165_02448-02449), suggesting that a capsular polysaccharide is formed, and were assigned to CPSS_FP accordingly.

**Vitamin and cofactor metabolism**

Based on the genome sequence, the microbe is unable to synthesize biotin, folic acid, nicotinic acid, pantothenic acid, and riboflavin, and should thus depend on external sources for these vitamins. A requirement for riboflavin was already demonstrated *in vitro* (9). It is

unclear whether *F. prausnitzii* can synthesize cobalamin (vitamin B12), as only 18 of about 30 enzymes necessary for cobalamin biosynthesis (10) are annotated.

Thiamine biosynthesis was incomplete in iFpraus_v0.1. We identified the missing genes manually and thus completed the pathway by including 4-amino-5-hydroxymethyl-2-methylpyrimidine synthetase (FAEPRAA2165_00647, BiGG ID: AHMMPS) and phosphomethylpyrimidine kinase (FAEPRAA2165_00779, BiGG IDs HMPK1, PMPK). To enable consumption of thiamine monophosphate, it was necessary to include thiamine phosphatase (BiGG ID: THMP) for modeling purposes.

iFpraus_v0.1 contained a reaction without supporting genomic evidence (3',5'-bisphosphate nucleotidase, BiGG ID: BPNT) that was added during automated gap-filling. The reaction is required to consume 3'-phosphoadenylyl sulfate (PAPS), as coenzyme A metabolism in the reconstruction would otherwise be nonfunctional. BPNT was thus included in the final reconstruction iFpraus_v1.0.

*F. prausnitzii* among other organisms possesses a selenophosphate synthase (11) (FAEPRAA2165_01593, BiGG ID: SELNPS) with unknown function. In *Enteroccocus faecalis*, selenophosphate is required for the activity of a reversible xanthine dehydrogenase (12). As *F. prausnitzii* possesses xanthine dehydrogenase (FAEPRAA2165_01590-01592, BiGG ID: r0502), a transporter for selenium and a demand reaction for selenophosphate were putatively included in the reconstruction.

Pyridoxal, thymidine and orotic acid were included in CDM2 medium, but not in CDM1 medium, which did not enable growth (Figure 1) and thus may be essential. However,

iFpraus_v0.1 was able to synthesize all three compounds. Pyridoxal phosphate could be synthesized due to a reaction (pyridoxine biosynthesis glutamine amidotransferase, BiGG ID: PLPS) filled in during the auto-completion step of the Model SEED pipeline. As this enzyme is not annotated, *F. prausnitzii* A2-165 most likely requires pyridoxal. PLPS was thus removed and a transporter for pyridoxal (FAEPRAA2165_02615, BiGG ID: PYDXabc) was included in the reconstruction.

**Carbon source utilization**

Pathways allowing utilization of glucose, fructose and maltose (6, 13) were already accounted for in the draft reconstruction. Generally, monosaccharides are imported into the cell either through a phosphotransferase system (PTS) or an ABC transporter. To enable galactose utilization (13), phosphoglucomutase (FAEPRAA2165_01951, BiGG ID: PGMT) was included.

A putative inulin degradation (13) pathway (assigned IDs INULINASE, INULINabc) was formulated based on the inulin utilization mechanism of the *Lachnospiraceae* representative *Roseburia inulinivorans*. It possesses a gene cluster containing an intracellular β-fructofuranosidase and an ABC transport system that are induced during growth on inulin. Inulin is internalized through the ABC system and degraded intracellularly (14). The closest matches in the *F. prausnitzii* genome to *R. inulinivorans* β-fructofuranosidase (FAEPRAA2165_02761, BLASTP score 470) and ABC transport system (FAEPRAA2165_02762-02764, BLASTP score 671, 418, and 436 respectively) were assigned to the pathway accordingly. The β-fructofuranosidase of *R. inulinivorans* is also effective against short-chain fructooligosaccharides (FOS), e.g., kestose. As *F. prausnitzii*

grows on FOS (6), appropriate reactions were formulated (assigned IDs KESTOASE, KESTOTTRASE, KESTOPTASE, KESTOabc, KESTOTTRabc, KESTOPTabc).

*F. prausnitzii* is able to ferment cellobiose (13), but does not possess β-glucosidase (6). We propose that cellobiose is either metabolized by cellobiose kinase (FAEPRAA2165_03524, BiGG ID: CELLBK) followed by 6-phospho-beta-glucosidase (FAEPRAA2165_00425, FAEPRAA2165_01165, BiGG ID: BGLA1), or by cellobiose phosphorylase (FAEPRAA2165_03089, BiGG ID: CEPA).

6-phospho-beta-glucosidase generally accepts arbutin and salicin as substrates (15) (BiGG IDs: 6PHBG, AB6PGH). However, no growth on salicin was observed (Table S1b). Accordingly, we did not identify a salicin transporter in the *F. prausnitzii* A2-165 genome.

*F. prausnitzii* A2-165 grows in starch solution (6), and potato starch (13). Two predicted cytosolic α-amylases are encoded in its genome (FAEPRAA2165_03210, FAEPRAA2165_02769). We thus constructed a pathway for soluble starch degradation in the cytosol (assigned IDs AMY1, O16G2).

Apple pectin, but not citrus pectin is utilized by *F. prausnitzii* (13). We propose that apple pectin is degraded extracellularly by a predicted extracellular polygalacturonase (FAEPRAA2165_02871) and a putative pectinesterase (FAEPRAA2165_00933) and included an appropriate reaction (assigned ID PECTIN_DEGe). The predicted growth rate on pectin as sole carbon source was higher for *F. prausnitzii* (0.21 hr-1) than for the *B. thetaiotaomicron* reconstruction (30) (0.16 hr-1 when growth on YCFA medium was simulated), in agreement

with the observation that *F. prausnitzii* can compete successfully with *B. thetaiotaomicron* over this carbon source (11).

Transporters for the fermentable carbohydrates galacturonate and glucuronate (13) are not annotated, and proton symport (BiGG ID: GALURt2r, GLCURt2r) was assumed. Uronic acid degradation is carried out by the subsystem of pentose phosphate pathway/ pentose and glucuronate interconversions and was already accounted for in iFpraus_v0.1.

Amino sugar (glucosamine, N-acetylglucosamine) utilization (13) pathways were already accounted for in iFpraus_v0.1. Transport of amino sugars was assumed via phosphotransferase system (PTS) as *F. prausnitzii* encodes a predicted N-acetylglucosamine-specific-PTS (FAEPRAA2165_00107, BiGG ID: GAMpts, ACGApts).

*F. prausnitzii* utilizes the N-acetylneuraminic acid (Table S1b) via N-Acetylneuraminate lyase (FAEPRAA2165_02440, BiGG ID: ACNML), N-acetylmannosamine 6-phosphate epimerase (FAEPRAA2165_02442, BiGG ID: AMANAPEr) and N-acetyl-D-mannosamine kinase (BiGG ID: AMANK, FAEPRAA2165_02443). Furthermore, we identified a sialic acid transporter (FAEPRAA2165_02437) that is colocalized with sialic acid utilization genes and is an ortholog of the SAT3-type transporter Spy_254 from Streptococcus pyogenes M1 GAS. A corresponding reaction (assigned ID ACNAMabc) was included.

The pentose moiety of inosine is predicted to be utilized for biomass production via purine-nucleoside phosphorylase (FAEPRAA2165_00956, FAEPRAA2165_01440) and the incomplete pentose phosphate pathway.

**Production of known secretion products**

The main secretion products of *F. prausnitzii* include butyrate, D-lactate, formate, and $CO_2$. L-lactate and hydrogen are not produced (6). The draft reconstruction was unable to produce and transport these compounds except $CO_2$. Transport reactions for formate, butyrate, and D-lactate were thus included (BiGG IDs: BUTtr, FORt, D_LACt2), though no associated genes could be identified.

Butyrate is the end product of *F. prausnitzii*'s central fermentation pathway as described above. Formate is generated by pyruvate formate lyase (FAEPRAA2165_02890-02891, BiGG ID: PFL). D-lactate is formed via D-lactate dehydrogenase (BiGG ID: LDH_D). An associated gene (FAEPRAA2165_01388) was identified (Table 3).

In the presence of fumarate, *F. prausnitzii* produces L-malate and succinate (5). A predicted C4-dicarboxylate transport cluster (FAEPRAA2165_01190-01193, BiGG IDs: FUMt, MAL_Lte, SUCCt) was assumed to transport L-malate, fumarate and succinate.

The draft reconstruction contained a quinone-, ferrichrome- and NADH-dependent L-lactate dehydrogenase. *F. prausnitzii* does not produce L-lactate (6). Genomic analysis revealed that the associated gene (dehydrogenase, FMN-dependent, FAEPRAA2165_01935) is misannotated and more similar to eukaryotic hydroxyacid oxidases (gene name *Hao2*, EC 1.1.3.15). The corresponding reaction (BiGG ID: GLYCTO4) was added and the previously included reactions (four in total) were removed.

**Remaining blocked reactions in the reconstruction**

While iFpraus_v0.1 contained 68% (618/904) blocked reactions, i.e., reactions including metabolites that can either be only produced or only consumed, iFpraus_v0.2 had 23% blocked reactions (225/997) (Table 1a). The pathways most affected by blocked reactions are cofactor and prosthetic

group biosynthesis and glycerophospholipid metabolism. In total, 39 reactions are blocked due to incompletely annotated pathways for vitamin B12 biosynthesis. In fact, 18 genes were present in the genome, while about 30 gene products are estimated to be required for vitamin B12 synthesis (25). Additional blocked reactions were in biotin biosynthesis (six genes present), folate biosynthesis (three genes present), quinone biosynthesis (two genes present), NAD biosynthesis (one gene present) and pantothenic acid biosynthesis (one gene present). In glycerophospholipid metabolism, 71 reactions are blocked, with 60 of them being linked to lysophospholipase L1 (FAEPRAA2165_02559) or phospholipase A2 (FAEPRAA2165_02521), since a phospholipid transporter could not be identified in the *F. prausnitzii* genome. It is thus unclear if *F. prausnitzii* A2-165 is able to take up and degrade phospholipids.

**Reconstruction improvement based on experimentally observed metabolite uptake and secretion**

Metabolite uptake and secretion was determined by mass spectrometry analysis for *F. prausnitzii* A2-165 cultures grown for 24 h. Samples taken at time points 0, 4, 8, 12, 16, 20 and 24h were analyzed. Furthermore, cell numbers were determined with FISH (Figure S1). Net metabolite uptake and secretion between 0h (medium before inoculation) and 20h was determined. Changes observed after 20h were not considered, as the culture was in stationary phase and concentration differences may be due to cell lysis. For all cases of statistically significant consumption or secretion, appropriate metabolites and reactions were added to the reconstruction to ensure that the observed metabolite consumption or secretion was captured. Metabolite uptake and secretion observed in experiment, as well as and metabolites and reactions included to connect these metabolites to the network are summarized in Table S2.

For unexpected secreted compounds, appropriate reactions and metabolites were included (Table S2) though secretion could only be determined qualitatively. For instance, N-acetyl-

glutamate is produced by N-acetylglutamate synthase (FAEPRAA2165_00167, BiGG ID: ACGS). This enzyme also accepts L-aspartate as substrate (15), resulting in N-acetyl-L-aspartate (BiGG ID: ACAS), which was also observed to be formed (Table S2). Phenyllactate is formed from phenylpyruvate by lactate dehydrogenase (encoded by *ldh* gene) in *Lactobacillus plantarum* (16). Thus, D-lactate dehydrogenase (FAEPRAA2165_01388) (Table 4) was putatively assigned to the corresponding reaction (BiGG ID: PLACOR).

Two metabolites could not be connected to the network and thus currently represent dead ends in the reconstruction. *F. prausnitzii* was observed to produce p-aminobenzoic acid in significant amounts (Table S2). However, biosynthesis of this vitamin precursor is not annotated in the *F. prausnitzii* genome. Similarly, pyridoxamine was significantly consumed by *F. prausnitzii*, but pyridoxamine 5'-phosphate oxidase is not annotated in its genome. It is currently unclear if, and how, these cofactors are converted to their active forms by this species. Finally, hydroxycaproic acid (Table S2) was not yet included in the reconstruction as its biosynthesis pathway in bacteria is currently unknown.

## Confidence score assignment

A confidence scoring system ranging from 1 to 4 was applied to iFpraus_v1.0, where 1 indicates that the reaction was included without evidence for modeling purposes only; 2 stands for either genetic annotation or physiological data support; 3 indicates support from transcriptomic data, and a score of 4 was given when the gene product has been isolated or characterized by enzyme assay. The confidence score is accumulative, e.g., genetic and physiological evidence add up to a confidence score of 4. The average confidence level was 2.29, indicating that on average there was at least either genomic or physiological support for the inclusion of metabolic and transport reactions in the reconstruction.

## Essential genes predicted by the model

We predicted the essentiality of genes included in iFpraus_v1.0 for growth on glucose minimal medium (constraints listed in Table S8) and rich medium. Deletion of essential genes results in a growth rate of zero. On glucose minimal medium, 176 out of 602 genes (29%) were predicted to be essential. The majority of these genes were involved in the biosynthesis of biomass precursors, in particular amino acid metabolism (28%) (Figure S2). As expected, gene essentiality in the *F. prausnitzii* reconstruction was lower in rich medium, as 84 genes (14%) were predicted to be essential under these conditions.

## Analysis of shadow prices calculated for the phenotypic phase planes

We performed a Phenotypic Phase Plane Analysis, where glucose was varied against acetate exchange while maximizing for biomass (see main text). We examined then the shadow prices for different metabolites for the entire phase plane. Based on the shadow prices, the phase plane can be divided into six phases (Figure S4a-b). In the first phase, glucose uptake was lowest and the model was carbon source-limited, as shown by positive shadow prices for glucose, while the shadow price for acetate was negative, meaning that the enforced acetate uptake reduced the growth rate as resources have to be allocated to metabolize the consumed acetate. In phase two to five, the shadow price for acetate became positive and increased substantially once the constraints switched from acetate uptake to acetate production. Glucose remained growth-limiting in phase two to five (Figure S4a-b). In the sixth phase, maximal growth rate was achieved. Notably, in phase six, growth was limited by the lack of e.g., $NAD^+$, $NADP^+$, FAD, ATP and acetyl-CoA (Figure S4c-g), while acetate, glucose and other carbon sources, e.g., pectins, had a shadow price of zero (Figure S4h). Further compounds limiting growth in phase six were identified as ammonia and other nitrogen sources, e.g. adenine, asparagine or N-acetylglucosamine (Figure S4i-l).

Furthermore, growth was limited in all phases by biomass precursors that can be either imported or synthesized *de novo*, e.g., arginine, histidine, lysine, phenylalanine, thiamin and uracil (Figure S4m-r).

Providing these cost-intensive biomass precursors to the simulated diet would thus enhance growth. For instance, one μmol of L-arginine costs one μmol of 2-oxoglutarate, seven μmol of ATP and four μmol each of $NADP^+$ and $NH_4$, and one μmol of lysine costs one μmol each of oxaloacetate and pyruvate, two μmol of ATP, four μmol of $NADP^+$ and two μmol of $NH_4$ (35). All of the required resources are growth-limiting in phase six (Figure S4m,o) and it would be beneficial for *F. prausnitzii* to take up readily available biosynthesis products. In agreement with this prediction, we observed a statistically significant uptake of arginine, histidine, lysine, phenylalanine, thiamin and uracil from CDM2 medium *in vitro* (Table S2). Building blocks of cell envelope biosynthesis, e.g. UDP-glucose, UDP-N-acetylglucosamine and UDP-N-acetylmuramic acid, also had positive shadow prices in phase six (Figure S4s-u). One μmol each of ATP and glucose-6-phosphate are required to make one μmol of UDP-glucose. The costs for UDP-N-acetylglucosamine and UDP-N-acetylmuramic acid are higher (one μmol each of fructose-6-phosphate, acetyl-CoA, $NH_4$ and three μmol of ATP for the former and one μmol each of fructose-6-phosphate, phosphoenolpyruvate, acetyl-CoA, $NADP^+$ and $NH_4$ and four μmol of ATP for the latter) (35). In agreement with these facts, the maximal shadow prices for UDP-N-glucosamine and UDP-N-acetylmuramic acid were higher (0.51 and 0.58) than for UDP-glucose (0.34) (Figure S4s-u).

Negative shadow prices were computed for metabolites involved in fatty acid metabolism (Figure S4v-w). Investing more resources than necessary in fatty acid biosynthesis is thus disadvantageous. Interestingly, some metabolites switched from positive to negative shadow prices in the different phases. For example, hexadecanoic acid had a positive shadow price in phase one to four, but a negative shadow price in phase five. Its production cost per μmol is eight μmol of acetyl-CoA, seven μmol of ATP and 14 μmol of $NADP^+$ (35). In phase one to four, saving these costs would thus be beneficial for *F. prausnitzii*, while in phase five, the metabolite would be in excess and costly to remove. Furthermore, N-2-acetyl-L-ornithine, a precursor of arginine, had a positive shadow price in phase six (optimal growth), but a negative shadow price in phase two to four (Figure S4x). During optimal growth, the model would thus benefit from increased availability of arginine precursors, while at suboptimal growth, the removal of excess N-2-acetyl-L-ornithine would consume resources.

## Supplemental Figures

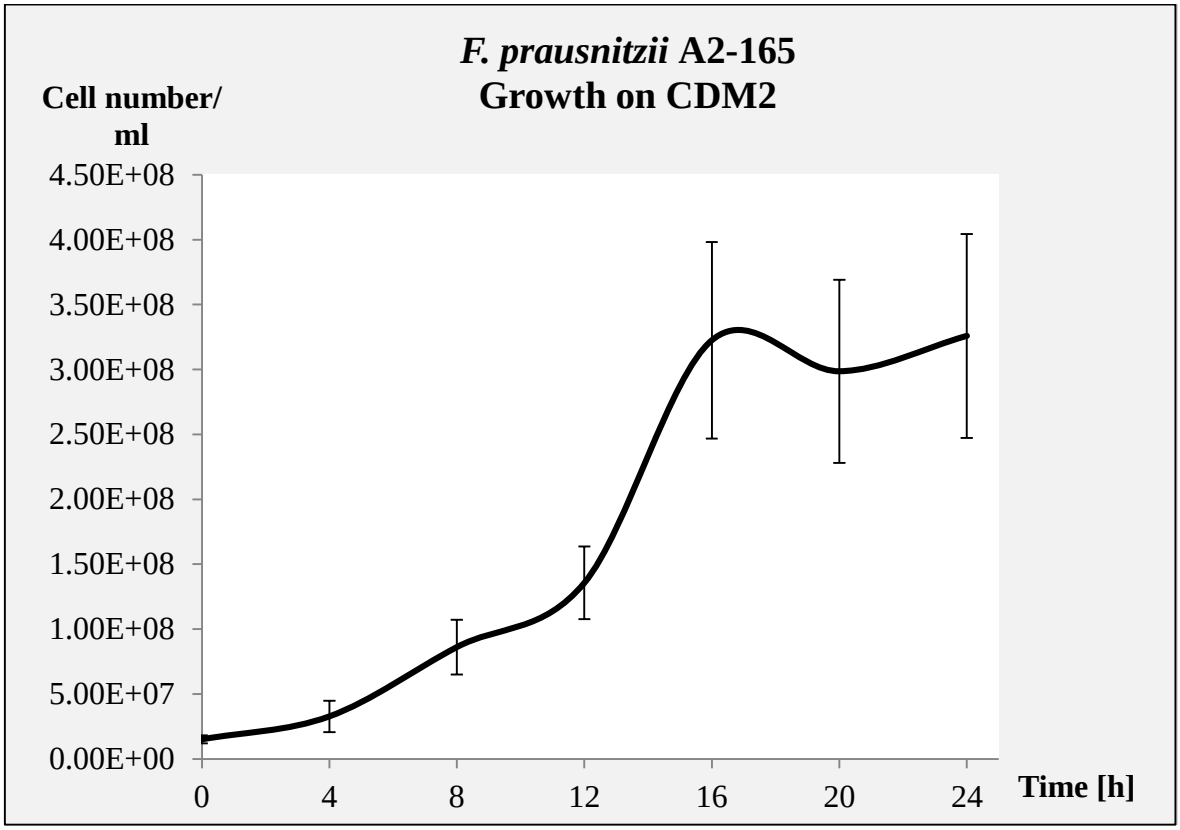


**Figure S1**: *F. prausnitzii* growth on chemically defined medium (CDM2) (composition in Table S10) during 24h. The growth curve represents the average of three biological replicates.

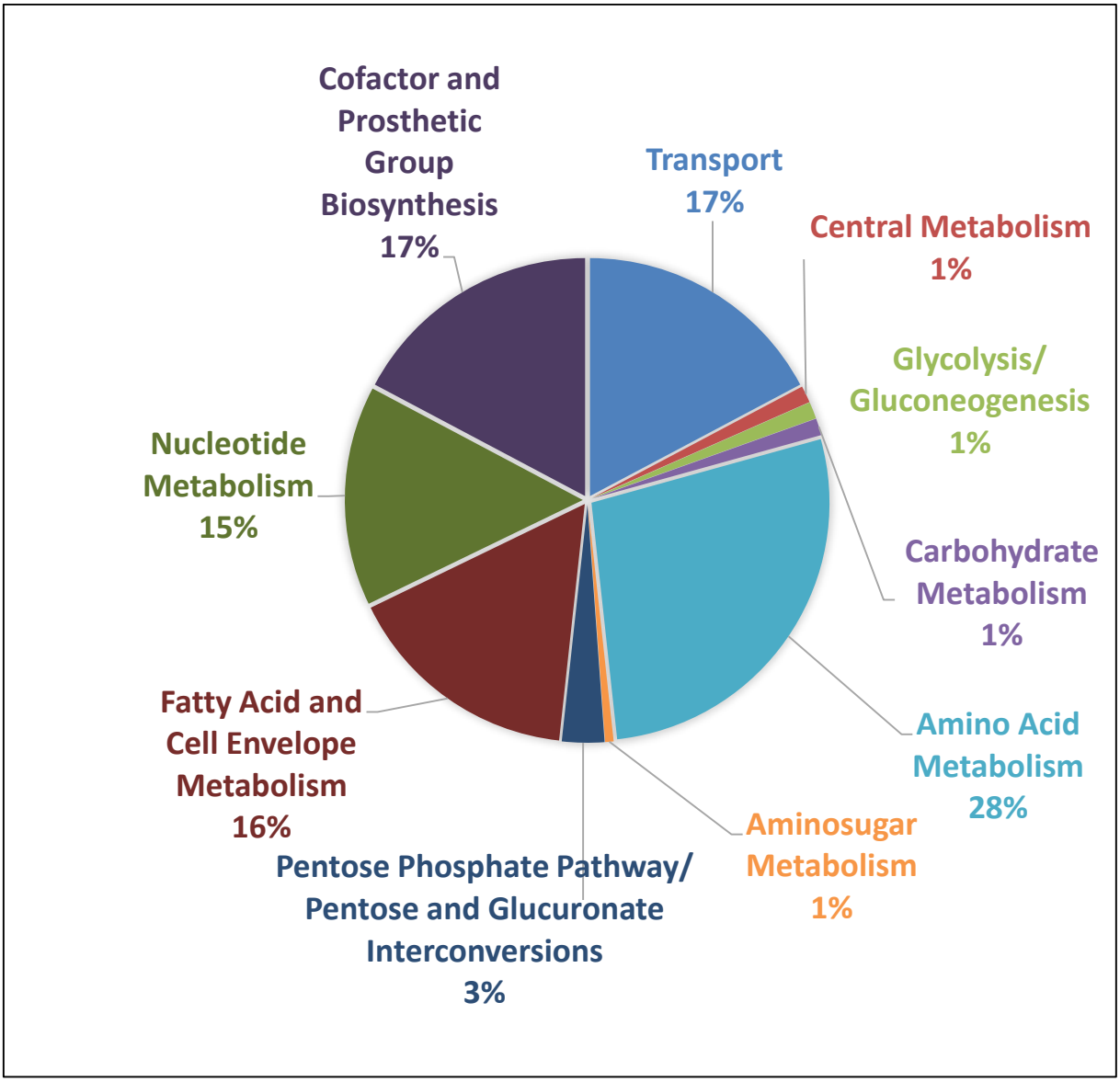


**Figure S2**: Subsystem participation of predicted essential genes for iFpraus_v1.0 on simulated glucose minimal medium.

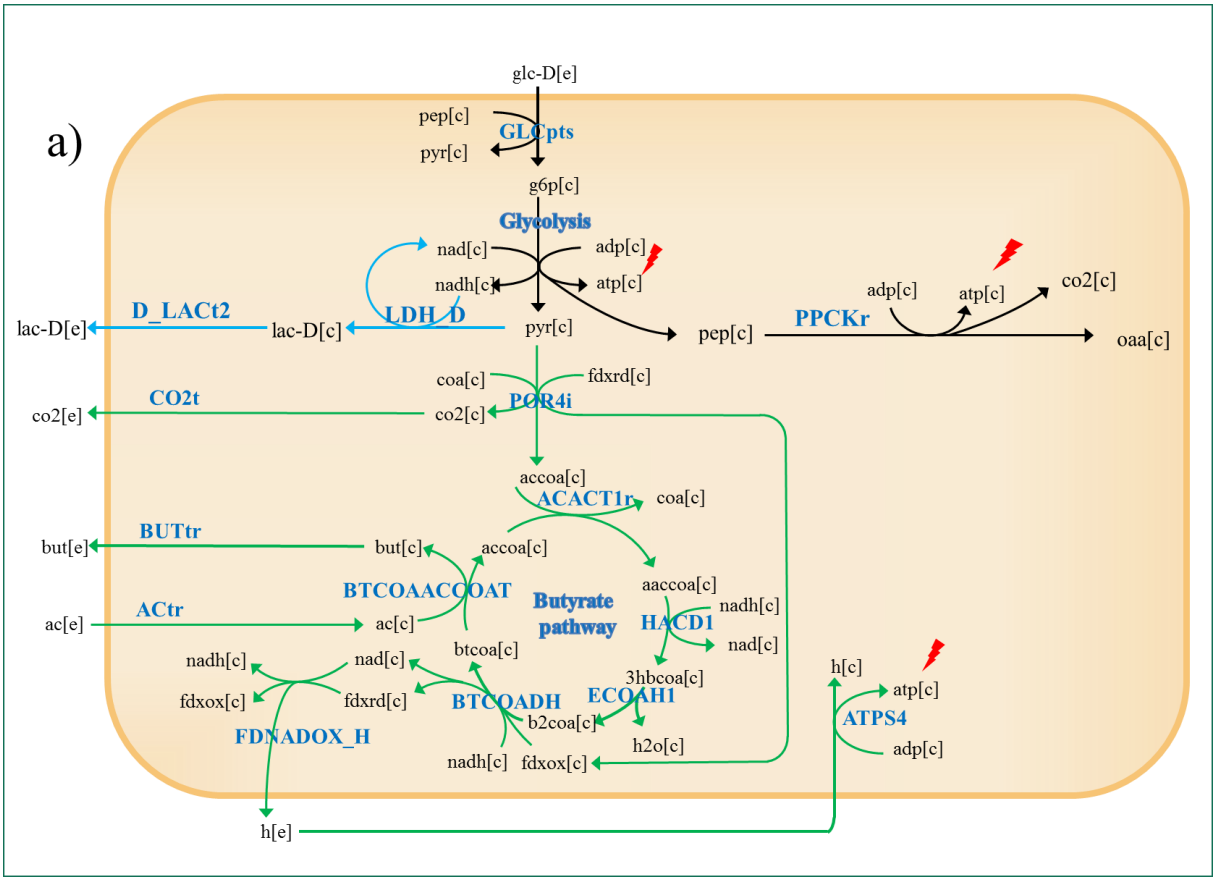


**Figure S3**: Pathway utilization in *F. prausnitzii*'s central metabolism predicted by iFpraus_v1.0.

a) Optimization for ATP maintenance while consuming glucose with and without acetate supply. Black arrows indicate reactions which carry flux under both conditions, blue arrows indicate reactions only active without acetate supply and green arrow shows reactions that only become active when acetate is provided. The red bolts indicating ATP-generating steps. For simplicity, intracellular protons and correct stochiometry are not represented in the figure.

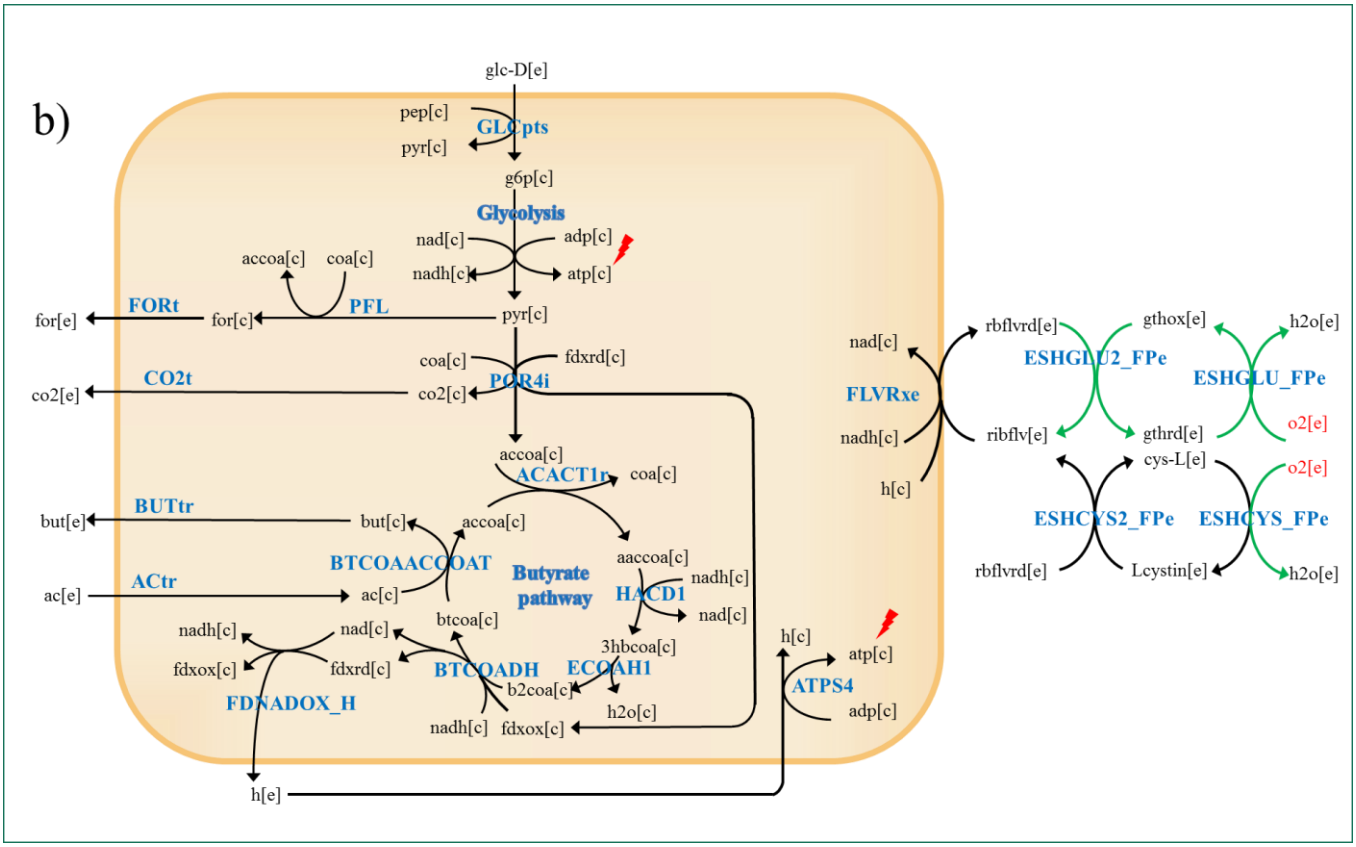


b) Optimization for biomass production on YCFAG medium with a glucose uptake rate of 10 mmol $gDw^{-1}.hr^{-1}$ (YCFAG10) and YCFAG medium with oxygen added as electron acceptor (YCFAG($O_2$)). Black lines illustrate reactions carrying flux under all three conditions and green arrows indicate reactions only active on YCFAG($O_2$) medium. The red bolts indicating ATP-generating steps. Entrance of oxygen into central metabolism is highlighted in red. For simplicity, intracellular protons and correct stochiometry are not represented in the figure.

Abbreviations: ACtr = acetate transport, ACACT1r = acetyl-CoA C-acetyltransferase, ACKr = acetate kinase, ATPS4 = ATP synthase, BTCOAACCOAT = butyryl-CoA:acetate CoA-transferase, BTCOADH = conversion of crotonoyl-CoA to butyryl-CoA by Bcd-Etf complex, BUTtr = but yrate transport, CO2t = $CO_2$ transport by diffusion, D_LACt2 = D-lactate transport, ECOAH1 = 3-hydroxyacyl-CoA dehydratase, ESHCYS_FPe / ESHCYS2_FPe = extracellular electron shuttle utilizing cysteine, ESHGLU_FPe / ESHGLU2_FPe =

extracellular electron shuttle utilizing glutathione, FDNADOX_H = ferredoxin:NAD oxidoreductase, FORt = formate transport, GLCpts = D-glucose transport via PEP:Pyr PTS, HACD1 = 3-hydroxyacyl-CoA dehydrogenase (acetoacetyl-CoA), LDH_D = lactate dehydrogenase, PFL = pyruvate formate lyase, POR4i = pyruvate:ferredoxin oxidoreductase, PPCKr = phosphoenolpyruvate carboxykinase, PTAr = phosphotransacetylase.

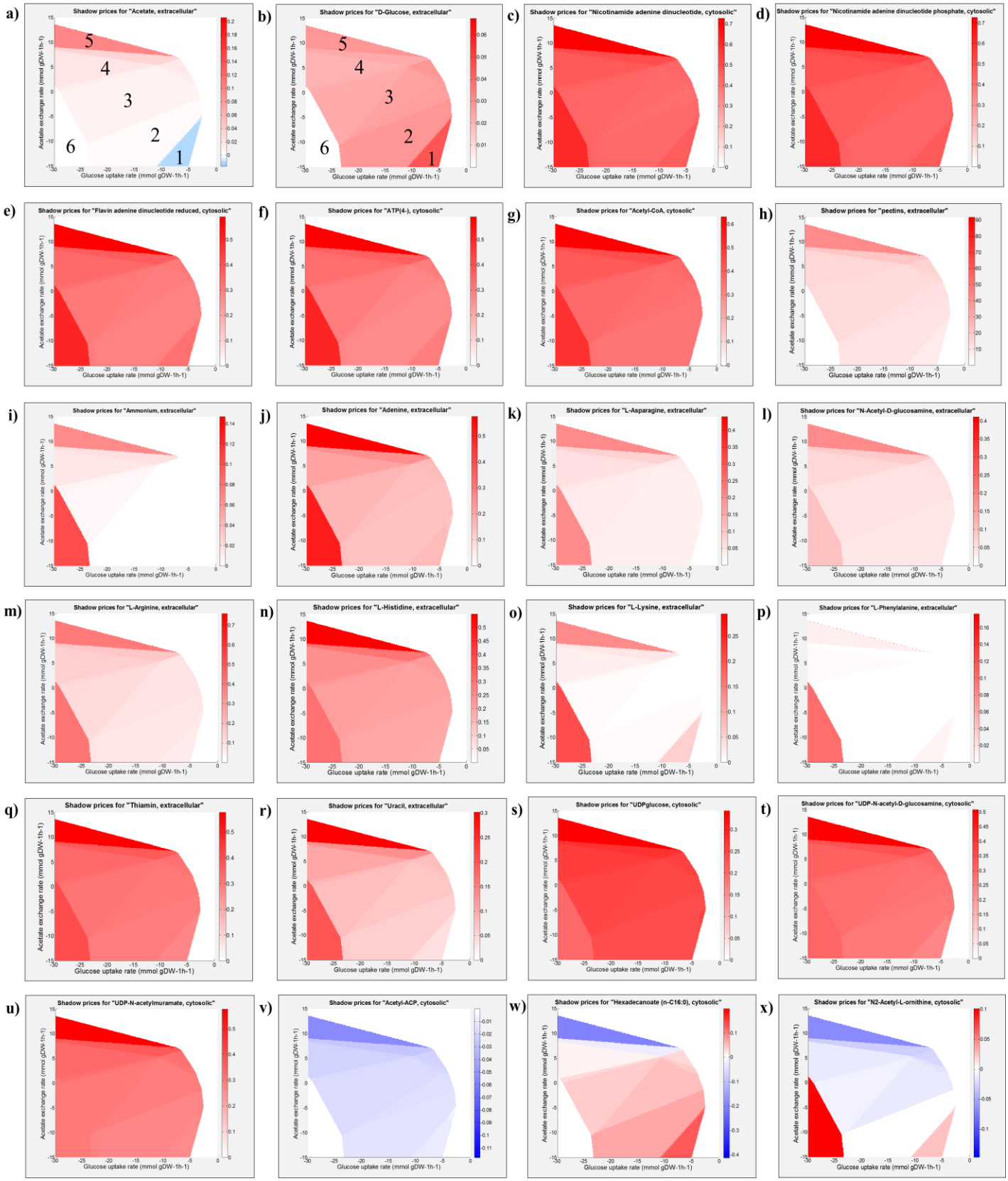


**Figure S4:** Shadow prices computed for a Phenotypic Phase Plane Analysis performed for the *F. prausnitzii* A2-165 reconstruction iFpraus_v1.0. Glucose and acetate uptake were varied while optimizing biomass production. The shadow prices for 24 metabolites were plotted as heat maps spanning the feasible solution space.

## Supplemental Tables

**Table S1**: Relative growth rates on known carbon sources with glucose as reference determined for iFpraus_v1.0 *in silico* and for *F. prausnitzii* A2-165 *in vivo* for growth on YCFA medium with carbon sources added one by one, and supporting references.

| **Carbon Source** | ***In silico*** **Relative growth rate** | ***In vivo*** **Relative growth rate** |
|---|---|---|
| Acetate | No growth | No growth (13) |
| Amino acids | No growth | No/ little growth (13) |
| Arabinogalactan | No growth | No growth (13) |
| Arabinose | No growth | No growth (6) |
| Cellobiose | 1.00 | 1.19 (13) |
| Chondroitin sulfate | No growth | No growth (13) |
| Fructose | 0.99 | Growth (6) (not determined quantitatively) |
| Fructooligosaccharides (kestose, kestotetaose, kestopentaose) | 0.89-0.94 | Growth (6) (not determined quantitatively) |
| Fucose | No growth | No growth (13) |
| Galactose | 0.55 | 1.51 (13) |
| Galacturonic acid | 0.77 | 0.40 (13) |

| | | |
|---|---|---|
| Glucosamine | 1.00 | 1.79 (13) |
| Glucose | 1.00 | 1.00 (13) |
| Glucose + fumarate | 1.47 | 1.59 (13) (calculated based on Table S1 in this reference) |
| Glucuronic acid | 0.77 | 1.57 (13) |
| Heparin | No growth | No growth (13) |
| Hyaluronic acid | No growth | No growth (13) |
| Inulin | 0.99 | 1.51 (13) |
| D-lactate | No growth | No growth (17) |
| Maltose | 0.78 | 1.17 (6) |
| Melibiose | No growth | No growth (6) |
| Mucin | No growth | No growth (13) |
| N-acetylglucosamine | 1.00 | 1.85 (13) |
| Pectin | 0.68 | 1.25 (13) |
| Raffinose | No growth | No growth (6) |
| Rhamnose | No growth | No growth (6) |
| Ribose | No growth | No growth (6) |
| Starch (solution) | 0.96 | 0.13 (6) |
| Sucrose | No growth | No growth (6) |

| | | |
|---|---|---|
| Trehalose | No growth | No growth (6) |
| Xylose | No growth | No growth (6) |

**Table S2**: Predicted biomass precursor auxotrophy and prototrophy and utilization as nitrogen and sulfur sources for *F. prausnitzii* A2-165. Predicted nitrogen and sulfur sources are highlighted in yellow.

**Table S3**: Comparison of assigned function for all genes included in the reconstruction with NCBI Protein, IMG, BioCyc and The Seed annotations. Genes for which a new annotation is proposed based on comparative genomics analysis are highlighted in yellow.

**Table S4**: Secretion products that may be produced by *F. prausnitzii* A2-165 *in vitro*, and model capabilities to synthesize them before and after curation based on metabolomic measurements.

| **Secretion product observed *in vitro*** | **Reference** | **iFpraus_v0.2** | **iFpraus_v1.0** |
|---|---|---|---|
| Butyric acid | (6) | Capable | Capable |
| Formic acid | (6) | Capable | Capable |
| D-lactic acid | (6) | Capable | Capable |
| Fumaric acid | Our study | Capable | Capable |
| Succinic acid | (5) | Capable | Capable |
| Malic acid | Our study, (5) | Capable | Capable |
| Dihydroorotic acid | Our study | Incapable | Capable |
| Glyceric acid | Our study | Incapable | Capable |
| Hypoxanthine | Our study | Capable | Capable |
| p-aminobenzoic acid | Our study | Incapable | Incapable |
| L-aspartic acid | Our study | Capable | Capable |
| L-glutamic acid | Our study | Capable | Capable |
| L-glutamine | Our study | Capable | Capable |
| L-threonine | Our study | Capable | Capable |
| 3-Methyl-2-oxovaleric acid | Our study | Incapable | Capable |

| | | | |
|---|---|---|---|
| Hydroxycaproic acid | Our study | Incapable | Capable |
| N-Acetyl-L-aspartic acid | Our study | Incapable | Capable |
| N-acetylglutamic acid | Our study | Incapable | Capable |
| Phenyllactic acid | Our study, (18) (strains SL3/3 and M21/2) | Incapable | Capable |

**Table S5**: Allowed flux spans of secretion products calculated *in silico* for iFpraus_v1.0 on anaerobic glucose (YCFAG10) medium and aerobic glucose (YCFAG ($O_2$)) medium (modeled after (26)). Fluxes/ concentrations with a negative sign indicate consumption. FVA was computed with 95% satisfaction of objective required.

| **Medium** | **YCFAG10** | **YCFAG ($O_2$)** |
|---|---|---|
| ***In silico* growth rate ($hr^{-1}$)** | 0.31 | 0.39 |
| **Acetate** | -15.95 to -7.80 | 9.58 to 16.55 |
| **Glucose** | -10 to -9.59 | -10 to -9.56 |
| **Fumarate** | 0 to 0.35 | 0 to 0.42 |
| **Butyrate** | 12.23 to 16.97 | 0 to 3.49 |
| **Formate** | 0 to 5.15 | 0 to 2.40 |
| **D-lactate** | 0 to 2.58 | 0 to 1.74 |
| **$CO_2$** | 15.78 to 21.93 | 17.43 to 22.51 |
| **$O_2$** | 0 | -18.54 to -10.67 |
| **Succinate** | 0 to 0.37 | 0 to 0.42 |
| **Malate** | 0 to 0.35 | 0 to 0.42 |

**Table S6:** Relation between flux through flavin reductase (assigned ID FVLRxe) and biomass production predicted by iFpraus_v1.0.

| **Simulation condition** | **Flux through FLVRxe (mmol $gDw^{-1}.hr^{-1}$)** | **Growth rate ($hr^{-1}$)** |
|---|---|---|
| YCFAG10 medium | 2.50 | 0.31 |
| YCFAG($O_2$) medium | 30.32 | 0.39 |
| YCFAG($O_2$) medium, flux through FLVRxe constrainted to zero | 0 | 0.30 |

**Table S7:** Description of reactions and metabolites included in the final reconstruction iFpraus_v1.0 in spreadsheet format.

**Table S8:** Simulation constraints for glucose minimal medium. Uptake of metabolites at a certain rate is allowed by constraining the lower bound of the respective exchange reaction to the corresponding negative value. For nutrients which are not provided in the simulated medium, the lower bund of exchange reactions is constrained to zero.

| **BiGG exchange reaction ID** | **Metabolite name** | **Uptake rate** **(mmol $g_{Dw}^{-1}.hr^{-1}$)** |
|---|---|---|
| EX_ac(e) | Acetate | 10 |
| EX_ala_L(e) | L-alanine | 1 |
| EX_btn(e) | Biotin | 0.1 |
| EX_ca2(e) | Calcium | 0.1 |
| EX_cbl1(e) | Cobalamin | 0.1 |
| EX_cl(e) | Chloride | 0.1 |
| EX_cobalt2(e) | Cobalt | 0.1 |
| EX_cu2(e) | Copper | 0.1 |
| EX_cys_L(e) | L-cysteine | 1 |
| EX_fe2(e) | Iron (II) | 0.1 |
| EX_fe3(e) | Iron (III) | 0.1 |
| EX_fol(e) | Folate | 0.1 |
| EX_glc(e) | Glucose | 10 |
| EX_k(e) | Potassium | 0.1 |

| | | |
|---|---|---|
| EX_mg2(e) | Magnesium | 0.1 |
| EX_met_L(e) | L-methionine | 1 |
| EX_nac(e) | Niacin | 1 |
| EX_nh4(e) | Ammonia | 5 |
| EX_pi(e) | Phosphate | 5 |
| EX_pnto_R(e) | Panthothenate | 0.1 |
| EX_pydx(e) | Pyridoxal | 0.1 |
| EX_ribflv(e) | Riboflavin | 0.1 |
| EX_ser_L(e) | L-serine | 1 |
| EX_so4(e) | Sulfate | 5 |
| EX_trp_L(e) | L-tryptophan | 1 |

**Table S9:** Simulation constraints for YCFA medium. Yeast extract was assumed to consist of all metabolites included in the yeast reconstruction iMM904 (19) that could also be transported by iFpraus_v1.0iFpraus_v1.0. Casitone was assumed to consist of all 20 amino acids. Uptake of metabolites at a certain rate is allowed by constraining the lower bound of the respective exchange reaction to the corresponding negative value. For nutrients which are not provided in the simulated medium, the lower bund of exchange reactions is constrained to zero. To simulate YCFAG medium, glucose uptake rate is set to -10 mmol $g_{Dw}^{-1}.hr^{-1}$.

| **BiGG exchange reaction ID** | **Metabolite name** | **Uptake rate** **(mmol $g_{Dw}^{-1}.hr^{-1}$)** |
|---|---|---|
| EX_ac(e) | Acetate | 33 |
| EX_ade(e) | Adenine | 1 |
| EX_ala_L(e) | L-alanine | 1 |
| EX_arg_L(e) | L-arginine | 1 |
| EX_asn_L(e) | L-asparagine | 1 |
| EX_asp_L(e) | L-aspartate | 1 |
| EX_btn(e) | Biotin | 1 |
| EX_ca2(e) | Calcium | 1 |
| EX_cbl1(e) | Cobalamin | 1 |
| EX_cl(e) | Chloride | 1 |
| EX_cobalt2(e) | Cobalt | 1 |

| | | |
|---|---|---|
| EX_cu2(e) | Copper | 1 |
| EX_cys_L(e) | L-cysteine | 1 |
| EX_fe2(e) | Iron (II) | 1 |
| EX_fe3(e) | Iron (III) | 1 |
| EX_fol(e) | Folate | 1 |
| EX_gln_L(e) | L-glutamine | 1 |
| EX_glu_L(e) | L-glutamate | 1 |
| EX_gly(e) | Glycine | 1 |
| EX_h2s(e) | Sulfide | 1 |
| EX_his_L(e) | L-histidine | 1 |
| EX_ile_L(e) | L-isoleucine | 1 |
| EX_k(e) | Potassium | 1 |
| EX_Lcystin(e) | L-cystine | 1 |
| EX_leu_L(e) | L-leucine | 1 |
| EX_lys_L(e) | L-lysine | 1 |
| EX_met_L(e) | L-methionine | 1 |
| EX_mg2(e) | Magnesium | 1 |
| EX_na1(e) | Sodium | 1 |
| EX_nac(e) | Niacin | 1 |

| | | |
|---|---|---|
| EX_nh4(e) | Ammonia | 1 |
| EX_phe_L(e) | L-phenylalanine | 1 |
| EX_pi(e) | Phosphate | 1 |
| EX_pnto_R(e) | Panthothenate | 1 |
| EX_pro_L(e) | L-proline | 1 |
| EX_ppa(e) | Propionate | 10 |
| EX_pydx(e) | Pyridoxal | 1 |
| EX_ribflv(e) | Riboflavin | 1 |
| EX_ser_L(e) | L-serine | 1 |
| EX_so4(e) | Sulfate | 1 |
| EX_thm(e) | Thiamin | 1 |
| EX_thr_L(e) | L-threonine | 1 |
| EX_trp_L(e) | L-tryptophan | 1 |
| EX_tyr_L(e) | L-tyrosine | 1 |
| EX_ura(e) | Uracil | 1 |
| EX_val_L(e) | L-valine | 1 |
| EX_xan(e) | Xanthine | 1 |

**Table S10:** Simulation constraints for CDM2 (expanded minimal medium). Uptake of metabolites at a certain rate is allowed by constraining the lower bound of the respective exchange reaction to the corresponding negative value. For nutrients which are not provided in the simulated medium, the lower bund of exchange reactions is constrained to zero.

| **BiGG exchange reaction ID** | **Metabolite name** | **Uptake rate** **(mmol $g_{Dw}^{-1}.hr^{-1}$)** |
|---|---|---|
| EX_ac(e) | Acetate | 33 |
| EX_ade(e) | Adenine | 1 |
| EX_ala_L(e) | L-alanine | 1 |
| EX_arg_L(e) | L-arginine | 1 |
| EX_asn_L(e) | L-asparagine | 1 |
| EX_asp_L(e) | L-aspartate | 1 |
| EX_btn(e) | Biotin | 1 |
| EX_ca2(e) | Calcium | 1 |
| EX_cbl1(e) | Cobalamin | 1 |
| EX_cl(e) | Chloride | 1 |
| EX_cobalt2(e) | Cobalt | 1 |
| EX_cu2(e) | Copper | 1 |
| EX_cys_L(e) | L-cysteine | 1 |
| EX_fe2(e) | Iron (II) | 1 |

| | | |
|---|---|---|
| EX_fe3(e) | Iron (III) | 1 |
| EX_fol(e) | Folate | 1 |
| EX_gln_L(e) | L-glutamine | 1 |
| EX_glu_L(e) | L-glutamate | 1 |
| EX_gly(e) | Glycine | 1 |
| EX_his_L(e) | L-histidine | 1 |
| EX_ile_L(e) | L-isoleucine | 1 |
| EX_k(e) | Potassium | 1 |
| EX_leu_L(e) | L-leucine | 1 |
| EX_lys_L(e) | L-lysine | 1 |
| EX_met_L(e) | L-methionine | 1 |
| EX_mg2(e) | Magnesium | 1 |
| EX_na1(e) | Sodium | 1 |
| EX_nac(e) | Niacin | 1 |
| EX_ncam(e) | Nicotinic acid | 1 |
| EX_nh4(e) | Ammonia | 1 |
| EX_phe_L(e) | L-phenylalanine | 1 |
| EX_pi(e) | Phosphate | 1 |
| EX_pnto_R(e) | Panthothenate | 1 |

| | | |
|---|---|---|
| EX_pro_L(e) | L-proline | 1 |
| EX_pydx(e) | Pyridoxal | 1 |
| EX_ribflv(e) | Riboflavin | 1 |
| EX_ser_L(e) | L-serine | 1 |
| EX_so4(e) | Sulfate | 1 |
| EX_thm(e) | Thiamin | 1 |
| EX_thr_L(e) | L-threonine | 1 |
| EX_trp_L(e) | L-tryptophan | 1 |
| EX_tyr_L(e) | L-tyrosine | 1 |
| EX_ura(e) | Uracil | 1 |
| EX_val_L(e) | L-valine | 1 |
| EX_xan(e) | Xanthine | 1 |

**Table S11:** Composition of CDM1 (initial minimal medium proposed by the model) per 1 l $H_2O$ bidest. The medium was sterile filtrated.

| **Compound** | **Concentration** |
|---|---|
| Glucose | 4.5 g/l |
| $NaHCO_3$ | 4 g/l |
| NaCl | 0.9 g/l |
| $K_2HPO_4$ | 0.45 g/l |
| $KH_2PO_4$ | 0.45 g/l |
| $CaCl_2$ * 2 $H_2O$ | 0.17 g/l |
| $MgSO_4$ * 7 $H_2O$ | 0.09 g/l |
| $MgCl_2$ | 0.16 g/l |
| $ZnSO_4$ | 0.004 g/l |
| $CuSO_4$ | 0.0024 g/l |
| $CoCl_2$ | 0.0002 g/l |
| $FeSO_4$ | 0.0056 g/l |
| $MnSO_4$ | 0.028 g/l |
| Sodium acetate | 2.7 g/l |
| Resazurin | 1 mg/l |
| Hemin | 10 mg/l |

| | |
|---|---|
| Cysteine (added to the tubes) | 1 g/l |
| Biotin | 10 µg/l |
| Cobalamin | 10 µg/l |
| 4-aminobenzoic acid | 30 µg/l |
| Folic acid | 50 µg/l |
| Pyridoxamine dihydrochloride | 150 µg/l |
| Riboflavin | 50 µg/l |
| Thiamin hydrochloride | 50 µg/l |
| Panthothenate | 50 µg/l |
| Nicotinic acid | 50 µg/l |
| Nicotinamide | 50 µg/l |
| L-alanine | 0.2375 g/l |
| L-methionine | 0.125 g/l |
| L-serine | 0.3375 g/l |
| L-tryptophan | 0.075 g/l |

**Table S12:** Composition of CDM2 (expanded chemically defined medium) per 1 l $H_2O$ bidest. The medium was sterile filtrated.

| **Compound** | **Concentration** |
|---|---|
| Glucose | 4.5 g/l |
| $NaHCO_3$ | 4 g/l |
| NaCl | 0.9 g/l |
| $K_2HPO_4$ | 0.45 g/l |
| $KH_2PO_4$ | 0.45 g/l |
| $CaCl_2$ * 2 $H_2O$ | 0.17 g/l |
| $MgSO_4$ * 7 $H_2O$ | 0.09 g/l |
| $MgCl_2$ | 0.16 g/l |
| $ZnSO_4$ | 0.004 g/l |
| $CuSO_4$ | 0.0024 g/l |
| $CoCl_2$ | 0.0002 g/l |
| $FeSO_4$ | 0.0056 g/l |
| $MnSO_4$ | 0.028 g/l |
| Sodium acetate | 2.7 g/l |
| Resazurin | 1 mg/l |
| Hemin | 10 mg/l |

| | |
|---|---|
| Cysteine (added to the tubes) | 1 g/l |
| Biotin | 10.01 mg/l |
| Cobalamin | 1.01 mg/l |
| 4-aminobenzoic acid | 10.03 mg/l |
| Folic acid | 1.05 mg/l |
| Pyridoxamine dihydrochloride | 5.015 mg/l |
| Riboflavin | 1.05 mg/l |
| Thiamin hydrochloride | 1.05 mg/l |
| Panthothenate | 1.05 mg/l |
| Nicotinic acid | 50 µg/l |
| Nicotinamide | 2.05 mg/l |
| Orotic acid | 5 mg/l |
| Thymidine | 5 mg/l |
| Pyridoxal-HCl | 2 mg/l |
| L-alanine | 0.475 g/l |
| L-serine | 0.675 g/l |
| L-phenylalanine | 0.75 g/l |
| L-tyrosine | 0.58 g/l |
| L-tryptophan | 0.15 g/l |

| | |
|---|---|
| L-glutamine | 0.39 g/l |
| L-asparagine | 0.35 g/l |
| L-arginine | 0.125 g/l |
| L-lysine | 0.4375 g/l |
| L-isoleucine | 0.2125 g/l |
| L-methionine | 0.125 g/l |
| L-threonine | 0.225 g/l |
| L-valine | 0.325 g/l |
| Glycine | 0.175 g/l |
| L-histidine | 0.15 g/l |
| L-leucine | 0.475 g/l |
| L-proline | 0.675 g/l |
| Adenine | 0.01 g/l |
| Uracil | 0.01 g/l |
| Xanthine | 0.01 g/l |
| Guanine hydrochloride | 0.01 g/l |

**Table S13:** Composition of CDM3 (curated chemically defined medium) per 1 l $H_2O$ bidest.

| **Compound** | **Concentration** |
|---|---|
| Glucose | 4.5 g/l |
| $NaHCO_3$ | 4 g/l |
| NaCl | 0.9 g/l |
| $K_2HPO_4$ | 0.45 g/l |
| $KH_2PO_4$ | 0.45 g/l |
| $CaCl_2$ * 2 $H_2O$ | 0.17 g/l |
| $MgSO_4$ * 7 $H_2O$ | 0.09 g/l |
| $MgCl_2$ | 0.16 g/l |
| $ZnSO_4$ | 0.004 g/l |
| $CuSO_4$ | 0.0024 g/l |
| $CoCl_2$ | 0.0002 g/l |
| $FeSO_4$ | 0.0056 g/l |
| $MnSO_4$ | 0.028 g/l |
| Sodium acetate | 2.7 g/l |
| Resazurin | 1 mg/l |
| Cysteine (added to the tubes)[1] | 1 g/l |
| Biotin | 10.01 mg/l |

| | |
|---|---|
| Cobalamin | 1.01 mg/l |
| Folic acid | 1.05 mg/l |
| Riboflavin | 1.05 mg/l |
| Thiamin hydrochloride | 1.05 mg/l |
| Panthothenate | 1.05 mg/l |
| Nicotinic acid | 50 µg/l |
| Nicotinamide | 2.05 mg/l |
| Thymidine | 5 mg/l |
| Pyridoxal-HCl | 2 mg/l |
| L-alanine | 0.475 g/l |
| L-serine | 0.675 g/l |
| L-phenylalanine | 0.75 g/l |
| L-tyrosine | 0.58 g/l |
| L-tryptophan | 0.15 g/l |
| L-arginine | 0.125 g/l |
| L-lysine | 0.4375 g/l |
| L-isoleucine | 0.2125 g/l |
| L-methionine | 0.125 g/l |
| L-histidine | 0.15 g/l |

| | |
|---|---|
| L-leucine | 0.475 g/l |
| L-proline | 0.675 g/l |
| L-valine | 0.325 g/l |
| Adenine | 0.01 g/l |
| Xanthine | 0.01 /l |

[1]Cysteine was not consumed significantly (Table S2) and thus may be nonessential, but is required as reducing agent in the medium.

## Supplemental References


1. **Henry CS, DeJongh M, Best AA, Frybarger PM, Linsay B, Stevens RL.** 2010. High-throughput generation, optimization and analysis of genome-scale metabolic models. Nat Biotechnol **28:**977-982.
2. **Schellenberger J, Park JO, Conrad TM, Palsson BO.** 2010. BiGG: a Biochemical Genetic and Genomic knowledgebase of large scale metabolic reconstructions. BMC Bioinformatics **11:**213.
3. **Duncan SH, Barcenilla A, Stewart CS, Pryde SE, Flint HJ.** 2002. Acetate utilization and butyryl coenzyme A (CoA):acetate-CoA transferase in butyrate-producing bacteria from the human large intestine. Appl Environ Microbiol **68:**5186-5190.
4. **Louis P, Flint HJ.** 2009. Diversity, metabolism and microbial ecology of butyrate-producing bacteria from the human large intestine. FEMS Microbiol Lett **294:**1-8.
5. **Khan MT, Duncan SH, Stams AJ, van Dijl JM, Flint HJ, Harmsen HJ.** 2012. The gut anaerobe Faecalibacterium prausnitzii uses an extracellular electron shuttle to grow at oxic-anoxic interphases. Isme J.
6. **Duncan SH, Hold GL, Harmsen HJ, Stewart CS, Flint HJ.** 2002. Growth requirements and fermentation products of Fusobacterium prausnitzii, and a proposal to reclassify it as Faecalibacterium prausnitzii gen. nov., comb. nov. Int J Syst Evol Microbiol **52:**2141-2146.
7. **Jantzen E, Hofstad T.** 1981. Fatty acids of Fusobacterium species: taxonomic implications. J Gen Microbiol **123:**163-171.
8. **Tsunashima H, Miyake K, Motono M, Iijima S.** 2012. Organization of the capsule biosynthesis gene locus of the oral streptococcus Streptococcus anginosus. J Biosci Bioeng **113:**271-278.
9. **Khan MT, Browne WR, van Dijl JM, Harmsen HJ.** 2012. How Can Faecalibacterium prausnitzii Employ Riboflavin for Extracellular Electron Transfer? Antioxid Redox Signal.

10. **Moore SJ, Warren MJ.** 2012. The anaerobic biosynthesis of vitamin B12. Biochemical Society transactions **40:**581-586.

11. **Zhang Y, Turanov AA, Hatfield DL, Gladyshev VN.** 2008. In silico identification of genes involved in selenium metabolism: evidence for a third selenium utilization trait. BMC Genomics **9:**251.

12. **Srivastava M, Mallard C, Barke T, Hancock LE, Self WT.** 2011. A Selenium-Dependent Xanthine Dehydrogenase Triggers Biofilm Proliferation in Enterococcus faecalis through Oxidant Production. J Bacteriol **193:**1643-1652.

13. **Lopez-Siles M, Khan TM, Duncan SH, Harmsen HJ, Garcia-Gil LJ, Flint HJ.** 2012. Cultured representatives of two major phylogroups of human colonic Faecalibacterium prausnitzii can utilize pectin, uronic acids, and host-derived substrates for growth. Appl Environ Microbiol **78:**420-428.

14. **Scott KP, Martin JC, Chassard C, Clerget M, Potrykus J, Campbell G, Mayer CD, Young P, Rucklidge G, Ramsay AG, Flint HJ.** 2011. Substrate-driven gene expression in Roseburia inulinivorans: importance of inducible enzymes in the utilization of inulin and starch. Proc Natl Acad Sci U S A **108 Suppl 1:**4672-4679.

15. **Kanehisa M, Araki M, Goto S, Hattori M, Hirakawa M, Itoh M, Katayama T, Kawashima S, Okuda S, Tokimatsu T, Yamanishi Y.** 2008. KEGG for linking genomes to life and the environment. Nucleic acids research **36:**D480-484.

16. **Jia J, Mu W, Zhang T, Jiang B.** 2010. Bioconversion of phenylpyruvate to phenyllactate: gene cloning, expression, and enzymatic characterization of D- and L1-lactate dehydrogenases from Lactobacillus plantarum SK002. Appl Biochem Biotechnol **162:**242-251.

17. **Duncan SH, Louis P, Flint HJ.** 2004. Lactate-utilizing bacteria, isolated from human feces, that produce butyrate as a major fermentation product. Appl Environ Microbiol **70:**5810-5817.

18. **Russell WR, Duncan SH, Scobbie L, Duncan G, Cantlay L, Calder AG, Anderson SE, Flint HJ.** 2013. Major phenylpropanoid-derived metabolites in the human gut can arise from microbial fermentation of protein. Molecular nutrition & food research **57:**523-535.

19. **Mo ML, Palsson BO, Herrgard MJ.** 2009. Connecting extracellular metabolomic measurements to intracellular flux states in yeast. BMC Syst Biol **3:**37.